

Semileptonic weak Hamiltonian to $\mathcal{O}(\alpha\alpha_s(\mu_{\text{Lattice}}))$ in momentum-space subtraction schemes

F Moretti¹, M Gorbahn¹, S Jäger² and E van der Merwe²

¹ Department of Mathematical Sciences, University of Liverpool, Liverpool L69 3BX, United Kingdom

² Department of Physics and Astronomy, University of Sussex, Falmer, Brighton BN1 9QH, United Kingdom

E-mail: Francesco.Moretti@liverpool.ac.uk, Martin.Gorbahn@liverpool.ac.uk, s.jaeger@sussex.ac.uk, ev95@sussex.ac.uk

Abstract. The CKM unitarity precision test of the Standard Model requires a systematic treatment of electromagnetic corrections for semi-leptonic decays. Electromagnetic corrections renormalize a semi-leptonic four-fermion operator and we calculate the $\mathcal{O}(\alpha\alpha_s)$ perturbative scheme conversion between the $\overline{\text{MS}}$ scheme and several momentum-space subtraction schemes, which can also be implemented on the lattice. We consider schemes defined by MOM and SMOM kinematics and emphasize the importance of the choice of projector for each scheme. The conventional projector, that has been used in the literature for MOM kinematics, generates an artificial QCD contribution to the conversion factor, which reflects in an unphysical dependence on the lattice matching scale. This can be traced to the violation of a Ward identity that holds in the case QED is neglected. We show how to remedy this by judicious choices of projector. The resulting Wilson coefficients (and operator matrix elements) have greatly reduced scale dependence.

1. Introduction

Leptonic and semi-leptonic decays of mesons, together with nuclear beta decays, provide a powerful tool for the extraction of CKM matrix elements [1], which results in an electroweak precision test of the standard model (SM) [2, 3].

The short-distance physics of meson and nuclear beta decays in the SM is described, to an excellent approximation, by an effective Hamiltonian that involves only a single charged-current operator

$$\mathcal{H}(x) = 4 \frac{G_F}{\sqrt{2}} V_{us}^* O(x), \quad O(x) = (\bar{s}(x)\gamma^\mu P_L u(x)) (\bar{\nu}_l(x)\gamma_\mu P_L l(x)), \quad (1)$$

where $P_L = (1 - \gamma^5)/2$ and G_F is the Fermi constant. At tree-level, the respective Wilson coefficient is directly proportional to G_F and a single CKM matrix element, here V_{us} . In particular, the measurements of Kaon [4] and nuclear beta decays [5] tests CKM unitarity in the first row, $\Delta_{CKM} = 1 - |V_{ud}^2| - |V_{us}^2| - O(|V_{ub}^2|) = 0$.

The extraction of the CKM matrix elements relies on the precise predictions of short distance QED and electroweak corrections, a determination of the relevant decay constants and form factors from lattice QCD [6] and the treatment of isospin breaking corrections and long distance QED effects using a combination of chiral perturbation theory and lattice field theory.

Traditionally, the calculation of the short distance contribution relies on current algebra and is performed in the W -mass renormalization scheme [7]. This scheme preserves the QED Ward identity and ensures that all weak corrections to the Fermi decay can be absorbed into G_F while the short distance corrections for the semi-leptonic decays comprise a large electromagnetic logarithm and electroweak corrections that are mostly absorbed into G_F . QED corrections for leptonic and semi-leptonic decays were calculated both in the current algebra approach [8], in chiral perturbation theory [9–11] or in a combined approach with chiral perturbation theory [12] where the electroweak box diagrams are calculated on the Lattice [13, 14].

Alternatively, the $\overline{\text{MS}}$ scheme, which is already used for the calculation of QED corrections [15, 16] to the Fermi theory that determine G_F as defined in Ref. [17], can be used. This scheme is also used for the calculation of electroweak corrections to the weak effective Hamiltonian [18], where the electroweak matching corrections and next-to-leading order anomalous dimensions for the operator O are given in Ref. [19]. In the $\overline{\text{MS}}$ scheme weak and hadronic scales are separated unlike in the W -mass scheme, and this scale separation simplifies the new physics interpretation and allows for a systematic inclusion of higher-order perturbative corrections.

The complete treatment of QED corrections on the lattice is a difficult task and has so far been performed for purely leptonic decays [20–23]. A novel feature in the semi-leptonic decay is that the relevant operator renormalizes in the presence of QED corrections. On the lattice, the renormalization is performed with momentum-space subtraction schemes, which can be implemented in continuum perturbation theory as well, thus allowing for a perturbative matching to the previously described schemes.

The renormalization in the RI'-MOM scheme with a lattice regulator was given in Ref. [22], including the one-loop perturbative matching to the W -mass scheme.

In our work [24], we perform the perturbative matching at two-loop level for different momentum-space subtraction schemes. These schemes are regulator-independent (RI) and are defined through a condition on a projected renormalized Green's function for a particular off-shell momentum configuration. As we show, the choice of projector is a crucial part of the definition of such schemes. In particular, special choices of projectors are required to ensure that the weak currents do not receive a finite renormalization [25, 26]. Similarly, it is preferable to choose renormalization conditions that do not result in a finite renormalization of the semi-leptonic operator O in the pure QCD limit, as a finite QCD renormalization would imply an artificial (residual) scale dependence that only (formally) disappears once all orders of perturbation theory are summed.

2. Renormalization conditions and change of scheme

Since the semi-leptonic operator O does not mix with other operators, any two schemes A, B differ only by a (finite) rescaling

$$O^A = C_O^{A \rightarrow B} O^B, \quad (2)$$

$$\psi_f^A = (C_f^{A \rightarrow B})^{1/2} \psi_f^B, \quad (3)$$

with ψ being the fermion field. Hence, the relation $C_O^B = C_O^{A \rightarrow B} C_O^A$ for the Wilson coefficient follows.

The RI schemes are defined by imposing the renormalization conditions

$$\sigma^A \equiv \frac{1}{4 p^2} \text{Tr} ((S^A)^{-1}(p) \not{\psi}) \stackrel{A \rightarrow \text{RI}}{=} 1 \quad (4)$$

and

$$\lambda^A \equiv \Lambda_{\alpha\beta\gamma\delta}^A \mathcal{P}^{\alpha\beta\gamma\delta} \stackrel{A \rightarrow \text{RI}}{=} 1 \quad (5)$$

at suitable kinematics, where \mathcal{P} is a constant Dirac tensor satisfying $\Lambda_{\alpha\beta\gamma\delta}^{(\text{tree})} \mathcal{P}^{\alpha\beta\gamma\delta} = 1$. Here, S is the connected fermion two-point function, while Λ is the amputated four-point function with O -insertion. It follows that the scheme conversion factors satisfy

$$\mathcal{C}_f^{A \rightarrow \text{RI}} = (\sigma^A)^{-1/2}, \quad (6)$$

$$\mathcal{C}_O^{A \rightarrow \text{RI}} = \lambda^A (\sigma_u^A \sigma_d^A \sigma_\ell^A)^{1/2}, \quad (7)$$

with implicit dependence on the choice of kinematic point and projector.

2.1. Specifics of the RI schemes and Ward identity

As introduced earlier, we focus on two RI schemes, eventually matched onto the $\overline{\text{MS}}$, namely:

- RI'-MOM [27];
- RI-SMOM [28].

The two schemes are characterised by different kinematics and projectors. In the RI'-MOM scheme, all the external momenta are equal, while RI-SMOM employs a symmetric configuration with two independent momenta such that

$$\text{RI}'\text{-MOM} : \quad p_1 = p_2 = p_3 = p_4 = p, \quad p^2 = -\mu^2, \quad (8)$$

$$\text{RI-SMOM} : \quad p_1 = p_3, \quad p_2 = p_4, \quad p_1^2 = p_2^2 = -\mu^2, \quad p_1 \cdot p_2 = -\frac{1}{2}\mu^2, \quad (9)$$

with (p_1, p_3) and (p_2, p_4) being the incoming and outgoing momenta respectively. In both schemes, the condition (4) is imposed.

In our work [24], we show that the conventional definition of the projector \mathcal{P} [29] entering the condition (5) on the renormalized four-point function leads, in contrast to what happens in the $\overline{\text{MS}}$, to a finite renormalization of the semi-leptonic operator even in the case QED is neglected. This can be traced to the violation of the QCD Ward identity (WI) for the quark current and it reflects in a scale dependence of the conversion factor. Such an artificial scale dependence is undesirable from a conceptual perspective and complicates error control when perturbative and lattice results are eventually combined.

To rectify this problem, we define a modified expression of the RI schemes, which rely on alternative expressions of \mathcal{P} . These $\overline{\text{RI}}$ schemes preserve the relations following from the Ward Identity, thus ensuring a trivial renormalisation of the operator and the absence of any pure QCD term in the conversion factor and, eventually, in the Wilson coefficient.

To better understand the main difference in our method, let us compare our definition of \mathcal{P} against the conventional one in the case of the simple MOM kinematics

$$\mathcal{P}^{\text{RI}'\text{-MOM}} = -\frac{1}{16}\gamma^\mu P_R \otimes \gamma_\mu P_R, \quad (10)$$

$$\mathcal{P}^{\overline{\text{RI}}\text{-MOM}} = \frac{1}{-12 p^2} \left(\not{p} P_R \otimes \not{p} P_R + \frac{p^2}{2} \gamma^\mu P_R \otimes \gamma_\mu P_R \right), \quad (11)$$

where $P_R = (1 + \gamma^5)/2$. We can see that in our newly derived projector there is an extra term that takes into account the presence of structures different than the one appearing at tree-level, namely $\not{p} P_R \otimes \not{p} P_R$. Neglecting QED, the amplitude can be written as $\Lambda = \Lambda^\mu(p) \otimes \gamma_\mu P_L + \mathcal{O}(\alpha)$, where $\Lambda^\mu(p) = F_1(p)\gamma^\mu P_L + F_2(p)\frac{p^\mu \not{p}}{p^2} P_L$. Yet, the WI only relates $F_1(p)$ to the fermion propagator. Using (11), however, it is possible to remove the terms proportional to $\not{p} P_L \otimes \not{p} P_L$, so that all loop corrections to the (projected) quark current will cancel against the field renormalization. This is not true, however, in the case when the conventional projector (10) is used. Then, $F_2(p)$ gives a non-zero contribution that is not cancelled by the field renormalization constant, which would lead to a finite renormalization of the quark current.

3. Results and numerics

The main goal of our work is the derivation of the two-loop conversion factors between continuum and lattice schemes. To this end, we computed the two-loop corrections in QED+QCD to the semi-leptonic operator. For all the details on the technicalities of our calculations, we refer the reader to Ref. [24]. The respective conversion factors between the $\overline{\text{MS}}$ and the $\overline{\text{RI}}\text{-MOM}$ and $\overline{\text{RI}}\text{-SMOM}$ schemes exhibit a scale dependence that mirrors the scale dependence of the relevant semi-leptonic Wilson coefficient. Working in renormalization group improved perturbation theory, this scale dependence will cancel order-by-order in perturbation theory for the product of the Wilson coefficient and a given conversion factor. By studying the residual scale dependence of this product, we can estimate the uncertainty from unknown higher-order corrections.

3.1. Scale dependence

Thanks to the employment of $\overline{\text{MS}}$ and the use of an EFT description of the electroweak theory, we can factorise the high scale (μ_W) and low scale (μ_L) contribution

$$\lambda_{\text{SM}}^i(p^2) = \overbrace{\lambda^i(\mu_L, p^2) C_O^{\overline{\text{MS}} \rightarrow i}}^{\text{low-scale}} \overbrace{\mathcal{U}(\mu_L, \mu_W) C_O^{\overline{\text{MS}}}}^{\text{high-scale}}(\mu_W) \quad (12)$$

so that altogether this expression is scale independent. Here, λ_{SM}^i is the full Standard Model amplitude. $\mathcal{U}(\mu_L, \mu_W)$ is the evolution kernel of the Wilson coefficient obtained solving the RGE. The value of the one- and two-loop anomalous dimension, together with the value of $C_O^{\overline{\text{MS}}}(\mu_W)$ can be found in [19]. The three-loop anomalous dimension $\gamma_W^{(2)}$ is unknown and thus left as a free parameter; we range it in a closed interval to estimate the uncertainties.

In the RI schemes, following (5), the expression (12) takes the expression

$$\lambda_{\text{SM}}^i(p^2) = C_O^i(p^2) = \mathcal{U}(\mu_L, \mu_W) C_O^{\overline{\text{MS}}}(\mu_W) C_O^{\overline{\text{MS}} \rightarrow i}(\mu_L, p^2) = C_\alpha^i + C_{\alpha_s}^i + \frac{\alpha}{4\pi} (C_{\alpha, \alpha_s \text{ LL}}^i + C_{\alpha, \alpha_s \text{ NLL}}^i), \quad (13)$$

where C_α^i and $C_{\alpha_s}^i$ are the resummed QED and leading QCD contributions, we recall that presence of the latter is a sign of the violation of the Ward Identity and it is absent in our formulation of the $\overline{\text{RI}}$ schemes. $C_{\alpha, \alpha_s \text{ LL}}^i$ and $C_{\alpha, \alpha_s \text{ NLL}}^i$ are the Leading-Log and Next-to-Leading-Log QCD contributions to the electromagnetic corrections.

3.2. RI'-MOM

For MOM kinematics we derive the operator conversion factor using both the conventional projector, comparing against the literature and finding a total agreement with the previous works at $O(\alpha)$ [22], and our new $\overline{\text{RI}}\text{-MOM}$ projector described in [24].

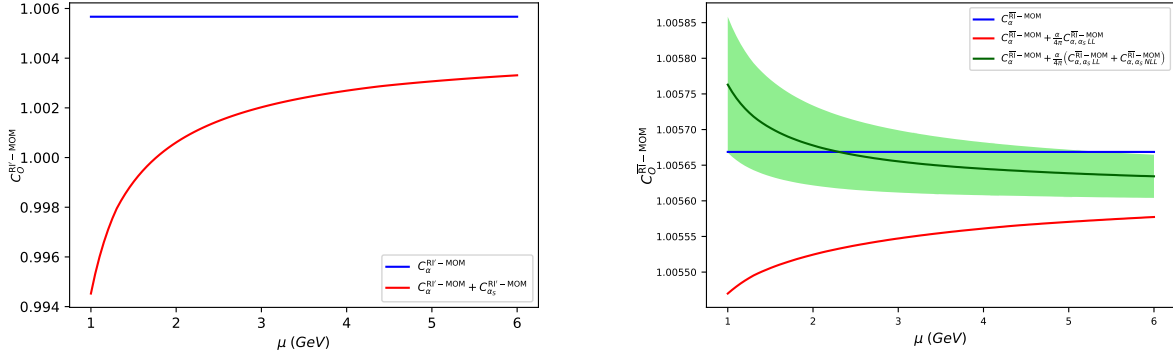


Figure 1: Residual scale dependence of the low-scale Wilson coefficient $C_O^{\text{RI}'\text{-MOM}}$ (left) and $C_O^{\text{RI-MOM}}$ with $\gamma_W^{(2)} = 0$ (dark green curve on the right). It is clear how the presence of pure QCD corrections introduces an artificial scale dependence. In contrast, we can see on the right the cancellation of the scale dependence in going from $C_{\alpha,\alpha_s\text{LL}}^{\text{RI-MOM}}$ to $C_{\alpha,\alpha_s\text{NLL}}^{\text{RI-MOM}}$, with a residual scale dependence now dramatically reduced. The light green shaded area shows the effect of the unknown value of $\gamma_W^{(2)}$ on the next-to-leading-log contribution: the upper limit is obtained with $\gamma_W^{(2)} = -100$, while the lower limit is given by $\gamma_W^{(2)} = 100$.

3.3. RI-SMOM

For the determination of the operator conversion factor in the SMOM kinematics we only consider our newly define scheme RI-SMOM [24]. Again, as in the MOM case, all the pure-QCD corrections cancel as expected.

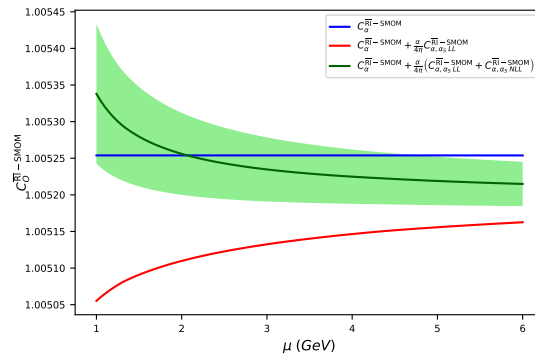


Figure 2: Residual scale dependence of the low-scale Wilson coefficient $C_O^{\text{RI-SMOM}}$ with our new projector, with $\gamma_W^{(2)} = 0$ (dark green curve). As in Figure 1, the residual scale dependence is suppressed by α . The light green shaded area shows the effect of the value of $\gamma_W^{(2)}$ on the NLL contribution: the top limit is obtained with $\gamma_W^{(2)} = -100$, while the bottom limit is given by $\gamma_W^{(2)} = 100$.

4. Conclusions

In our paper we have calculated the scheme conversions for the semi-leptonic weak effective operator between the $\overline{\text{MS}}$ scheme and the $\overline{\text{RI}}\text{-MOM}$ and $\overline{\text{RI}}\text{-SMOM}$ schemes. We emphasized the importance of the projector in the definition of the scheme and found that a conventional choice of projector leads to an artificial QCD correction to the conversion factor with a bad perturbative convergence. Using the Ward identity in the pure-QCD limit, we defined modified schemes that rectify this problem, by showing the existence of adequate new projectors. Performing an effective field theory analysis with renormalization-group-improved perturbation theory we showed that these schemes indeed exhibit an excellent perturbative convergence, when LL and partial NLL QCD corrections were added to the photonic corrections. Given the theoretical attractiveness and good perturbative convergence, we argue that the schemes defined with our proposed projectors should be used in future work on semileptonic decays in place of the conventional RI schemes. In particular, this should allow a better precision in determining CKM matrix elements in future phenomenological analyses. Our approach also lends itself to a systematic improvement of short-distance contributions.

References

- [1] Bazavov A *et al.* (Fermilab Lattice, MILC) 2019 *Phys. Rev. D* **99** 114509 (*Preprint hep-lat/1809.02827*)
- [2] Cirigliano V, Jenkins J and Gonzalez-Alonso M 2010 *Nucl. Phys. B* **830** 95–115 (*Preprint hep-ph/0908.1754*)
- [3] Crivellin A and Hoferichter M 2020 *Phys. Rev. Lett.* **125** 111801 (*Preprint hep-ph/2002.07184*)
- [4] Estrada Tristan N P (Na62) 2019 *PoS LHCP2019* 040
- [5] Algora A, Tain J L, Rubio B, Fallot M and Gelletly W 2021 *Eur. Phys. J. A* **57** 85 (*Preprint nucl-ex/2007.07918*)
- [6] Aoki Y *et al.* (Flavour Lattice Averaging Group (FLAG)) 2022 *Eur. Phys. J. C* **82** 869 (*Preprint 2111.09849*)
- [7] Sirlin A 1982 *Nucl. Phys. B* **196** 83–92
- [8] Sirlin A 1978 *Rev. Mod. Phys.* **50** 573 [Erratum: *Rev. Mod. Phys.* **50**, 905 (1978)]
- [9] Knecht M 1995 *Nuclear Physics B - Proceedings Supplements* **39** 249–252
- [10] Knecht M, Neufeld H, Rupertsberger H and Talavera P 2000 *The European Physical Journal C* **12** 469–478
- [11] Neufeld H and Rupertsberger H 1996 *Zeitschrift für Physik C: Particles and Fields* **71** 131–138
- [12] Seng C Y, Galviz D and Meißner U G 2020 *JHEP* **02** 069 (*Preprint hep-ph/1910.13208*)
- [13] Ma P X, Feng X, Gorchtein M, Jin L C and Seng C Y 2021 *Phys. Rev. D* **103** 114503 (*Preprint hep-lat/2102.12048*)
- [14] Feng X, Gorchtein M, Jin L C, Ma P X and Seng C Y 2020 *Physical Review Letters* **124**
- [15] van Ritbergen T and Stuart R G 2000 *Nucl. Phys. B* **564** 343–390 (*Preprint hep-ph/9904240*)
- [16] Steinhauser M and Seidensticker T 1999 *Phys. Lett. B* **467** 271–278 (*Preprint hep-ph/9909436*)
- [17] Workman R L (Particle Data Group) 2022 *PTEP* **2022** 083C01
- [18] Gambino P and Haisch U 2001 *JHEP* **10** 020 (*Preprint hep-ph/0109058*)
- [19] Brod J and Gorbahn M 2008 *Phys. Rev. D* **78** 034006 (*Preprint hep-ph/0805.4119*)
- [20] Carrasco N, Lubicz V, Martinelli G, Sachrajda C T, Tantalo N, Tarantino C and Testa M 2015 *Phys. Rev. D* **91** 074506 (*Preprint hep-lat/1502.00257*)
- [21] Giusti D, Lubicz V, Martinelli G, Sachrajda C T, Sanfilippo F, Simula S, Tantalo N and Tarantino C 2018 *Phys. Rev. Lett.* **120** 072001 (*Preprint 1711.06537*)
- [22] Di Carlo M, Giusti D, Lubicz V, Martinelli G, Sachrajda C T, Sanfilippo F, Simula S and Tantalo N 2019 *Phys. Rev. D* **100** 034514 (*Preprint hep-lat/1904.08731*)
- [23] Boyle P A, Guelpers V, Juettner A, Lehner C, hOgain F O, Portelli A, Richings J P and Sachrajda C T 2019 *PoS LATTICE2018* 267 (*Preprint 1902.00295*)
- [24] Gorbahn M, Jäger S, Moretti F and van der Merwe E 2022 (*Preprint hep-ph/2209.05289*)
- [25] Gracey J 2003 *Nuclear Physics B* **662** 247–278
- [26] Gracey J A 2011 *The European Physical Journal C* **71**
- [27] Martinelli G, Pittori C, Sachrajda C T, Testa M and Vladikas A 1995 *Nucl. Phys. B* **445** 81–108 (*Preprint hep-lat/9411010*)
- [28] Sturm C, Aoki Y, Christ N H, Izubuchi T, Sachrajda C T C and Soni A 2009 *Physical Review D* **80** ISSN 1550-2368
- [29] Garron N 2018 *EPJ Web Conf.* **175** 10005